

## 5 Competing Dissociation Channels and Branching Ratios in the Photolysis of SOCl<sub>2</sub> at 235 nm

The photodissociation of thionyl chloride (SOCl<sub>2</sub>) at 235 nm has been studied by 3D imaging of the chlorine product in its ground state <sup>2</sup>P<sub>3/2</sub> [Cl] and excited spin-orbit state <sup>2</sup>P<sub>1/2</sub> [Cl\*] employing the resonance enhanced multi-photon ionization and time-of-flight technique (REMPI-TOF). Upon excitation at 235 nm, SOCl<sub>2</sub> predominantly undergoes dissociation via the two channels: (5.1) SOCl + Cl and (5.2) SO + 2Cl. The relative yield of channel (5.1) with respect to channel (5.2) was determined to be 3.5:1. The total yield of Cl\*,  $\phi(\text{Cl}^*) = P(\text{Cl}^*)/[P(\text{Cl}) + P(\text{Cl}^*)]$ , was found to be 0.35. The obtained speed distributions of Cl and Cl\* are bimodal and exhibit a different behavior for the different spin-orbit states. The dependence of the anisotropy parameter  $\beta$  on the fragment speed was directly determined by a novel 3D imaging technique. For both spin-orbit states the anisotropy parameter differs clearly for fast and slow chlorine atoms, where a pronounced change from the  $\beta$  value of  $\sim 0.75$  to a value close to zero at about 2000 m/s is observed. Slow chlorine atoms are released almost isotropically and predominantly in the ground state whereas fast chlorine atoms have an anisotropy parameter close to the theoretically limiting value and are distributed almost equally between ground and excited state Cl. These observations can be explained by two competing mechanisms: The first one releases SOCl and one fast chlorine atom in a fast process characterized by the non-vanishing positive  $\beta$  parameter and a lifetime of less than 200 fs via an excited state of A'' symmetry. The second manifests itself both as a three-body decay producing two chlorine atoms and one SO molecule and as a two-body decay generating a Cl atom in conjunction with an internally excited SOCl\* radical via an A' excited potential energy surface.

### 5.1 Introduction

The implication of a novel 3D imaging technique that allows to monitor the full three-dimensional momentum vectors of individual products of a chemical elementary reaction<sup>1</sup> has led to the reexamination of the ultraviolet photodissociation of a series of tetratomic molecules which can, in principle, decay into three fragments. Adequate projection methods allow to extract state-specific fragment kinetic energy distributions as well as the

anisotropy parameter  $\beta$  describing the spatial fragment distribution from the 3D momentum data. Especially the determination of the speed dependence of the anisotropy parameter proved to be useful in the analysis of competing two- and three-body channels in the photodissociation of CSeCl<sub>2</sub><sup>2</sup> and COCl<sub>2</sub><sup>3,4</sup>. As part of a series about the photodissociation of structurally similar molecules we present here a study of the photofragmentation of the thionyl chloride (SOCl<sub>2</sub>) molecule. Other than in the above mentioned studies, here a different electronic transition leads to a direct excitation of the dissociation coordinate for the same dissociation energy.

The UV photolysis of the SOCl<sub>2</sub> molecule has been subject of several experimental investigations. The absorption spectrum is smooth and starts around 300 nm with distinct shoulders at 244 nm and 194 nm, as shown in Fig. 5.1.<sup>5</sup> It has tentatively been assigned to at least four partially overlapping electronic excitations from non-bonding electrons at the S and the Cl atoms to both anti-bonding  $\pi^*_{\text{SO}}$  and  $\sigma^*_{\text{S-Cl}}$  orbitals.<sup>6</sup>

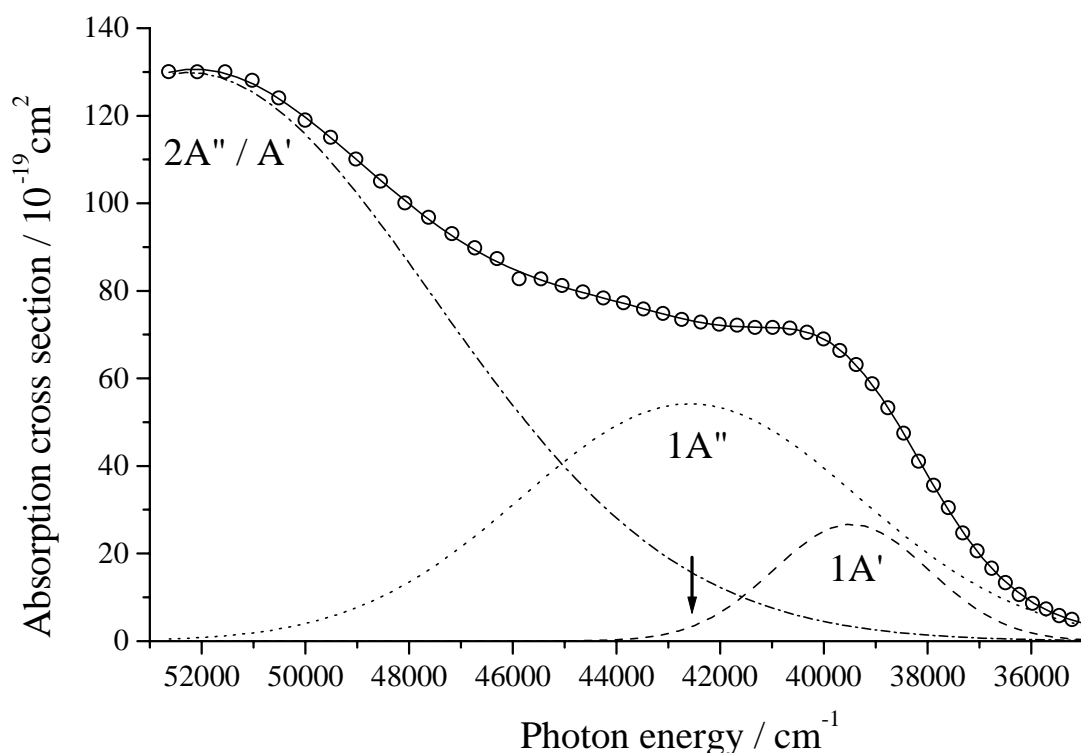


**Figure 5.1:** Absorption spectrum of SOCl<sub>2</sub>. Experimental data are taken from Uthmann.<sup>5</sup> The first maximum at 250 nm has been assigned to a  $\pi^*_{\text{SO}} \leftarrow n_{\text{S}}$  transition from a non-bonding lone pair electron on the sulfur atom to the anti-bonding  $\pi^*$  molecular orbital of the S-O bond. The second maximum below 200 nm

has been considered to result from  $n_S$  or  $n_{Cl}$  excitation to either the anti-bonding  $\sigma^*_{S-Cl}$  or  $\pi^*_{S-O}$  orbitals. Tuning the dissociation wavelength between the two maxima should result in competing dissociation mechanisms originating from the respective excited states. Three Gaussians are fitted to the spectrum in order to elucidate the contributions of the different states. The dashed line is assigned to the  $\pi^* \leftarrow n_S$  transition, the dotted line to the  $\sigma^*_{S-Cl} \leftarrow n_S$ . Due to the large numbers of possible transitions from the  $n_{Cl}$  orbitals no assignment could be made below 200 nm. The excitation wavelength is marked by an arrow.

The first photodissociation experiments were performed by Donovan<sup>7</sup> et al in 1969. They used flash photolysis in the UV region ( $\lambda \geq 185$  nm) to explore the photodecomposition of SOCl<sub>2</sub>. The observed photoproducts were ground state Cl and excited SOCl\* partner fragments. Therefore they proposed that the primary process is the fission of one sulfur-chlorine bond and that the excited SOCl\* may undergo unimolecular decomposition to SO and Cl or may relax to the ground state SOCl. More recently, Kawasaki and co-workers<sup>8</sup> investigated the photofragmentation of SOCl<sub>2</sub> in a molecular beam by photofragment translational spectroscopy (PTS). Using 193 nm excitation, they found that the radical channel (5.1):



is operative in competition with the three-body decay<sup>9</sup> (5.2):



On the basis of simulation they concluded that the three-body decay occurs mainly via an asynchronous concerted mechanism and a sequential decay is of minor importance. At 248 nm it was found that the photodissociation proceeds via the radical (5.1) and the molecular channel (5.3):



with the former dominating the latter.

Detailed examinations of the decay of SOCl<sub>2</sub> at 248 nm and 193 nm were performed by Baum et al.<sup>10</sup> using PTS in 1992. In agreement with Kawasaki they observed at 248 nm a decay via channel (5.1) and (5.3), whereas a three-body decay along channel (5.2) could not be observed although it is energetically possible. The molecular channel (5.3) which was of minor importance (3,5 %) yields mainly Cl<sub>2</sub> ( $X^1\Sigma_g^+$ ) and SO ( $b^1\Sigma^+$ ) and to a lesser extent Cl<sub>2</sub> ( $X^1\Sigma_g^+$ ) and SO ( $X^3\Sigma^-$ ). The anisotropy parameter  $\beta_{Cl_2}$  for the molecular decay was found to be  $0.7 \pm 0.1$  which hints at a decay on a surface of A' symmetry. In the case of the radical channel (5.1) the observed  $\beta_{Cl}$  value was  $0.8 \pm 0.1$  which indicated that the decay occurs on a surface of A'' symmetry and is fast and direct. Thus, at the excitation wavelength of 248 nm two surfaces are overlapping. At 193 nm Baum et al. observed three competing decay channels, where the yields are 17 %, 3 %, and 80 % for the radical channel, the molecular channel, and the three-body decay, respectively. The released SOCl partner fragment in the radical channel was found with an average excitation of 109 kJ/mol, and the observed  $\beta_{SOCl}$  parameter was found to be  $0.40 \pm 0.05$ . The decay mechanism of the three-body decay was suggested to be asynchronous concerted whereas a sequential decay and secondary photolysis could be excluded. Simulations led to a calculated  $\beta_{SO}$  value of -0.5 and of 0.33 for  $\beta_{SOCl}$  which are in good agreement with the measured  $\beta_{SO}$  of -0.65 and the  $\beta_{SOCl}$  value in the radical channel of 0.4.

In 1993 Weiner and co-workers studied the photolysis of SOCl<sub>2</sub> at 193 nm and 248 nm where they concentrated on the vibrational and rotational distribution of the SO ( $X^3\Sigma^-$ ) fragments which was monitored by laser induced fluorescence (LIF). At 248 nm the vibrational distribution was found to be bimodal, which was explained by a competition of the sequential three-body decay (5.2) and the molecular decay channel (5.3). At 193 nm, the inverted vibrational distribution hinted at a fast decay on the populated surface confirming the assumption of the concerted three-body decay. Their results were supported by microwave studies of the SO fragment performed by Bogey et al.<sup>11</sup>

In spite of the previous examinations there are still unanswered questions which concern the nature and the contribution of the excited states at 248 nm as well as the spin-orbit state distribution of SO and Cl which cannot be detected by PTS. The state selective spatial fragment distribution yields detailed information about the dynamics of the decay process. In 1996 Kawasaki et al.<sup>12</sup> performed the first state and energy sensitive experiments on the

photodissociation of SOCl<sub>2</sub> at 235 nm via ion-imaging. They concluded that both reaction channels (5.1) and (5.2) are present. The observed Cl\* atoms clearly have a much higher kinetic energy than the Cl atoms. The Cl atoms are isotropically distributed ( $\beta_{Cl} \approx 0$ ), only the  $\beta$  parameter for the high kinetic energy region was  $0.7 \pm 0.2$ . These observations are in good agreement with the results obtained by Baum et al.<sup>10</sup> and by Roth et al.<sup>6,13</sup> Roth et al. performed state and energy sensitive experiments on the photodissociation of SOCl<sub>2</sub> at 235 nm via REMPI-TOF where Cl atoms were produced via the radical and the three-body decay channel. In the case of the radical channel, the Cl atoms were released in the spin-orbit ground and excited state with the same probability. 50 % of the available energy was found as internal energy in the SOCl partner fragment. An electronic excitation as postulated by Baum et al. seems unlikely since recent ab initio calculations do not yield a low lying state in the energy range under consideration.<sup>14</sup> The radical channel is likely to occur via the ( $\sigma_{S-Cl}^*(a'') \leftarrow n_S(a')$ ) transition, which was suggested due to the observed  $\beta_{Cl}$  parameter of 0.8. In the case of the three-body decay, the SO molecules were found to be vibrationally excited up to  $v''=1$  and rotationally excited. The observed SO molecules were released mainly via the three-body decay, whereas the contribution of the molecular channel was negligible. The Cl atoms which were produced in the three-body decay were mainly released in the spin-orbit ground state (88%). A synchronous concerted decay mechanism could be excluded from simulations to the kinetic energy distribution, whereas both an asynchronous concerted decay and a sequential decay could describe the results well. A set of two discrete  $\beta_{Cl}$  parameters were obtained from a forward convolution procedure simulating the observed TOF profiles. The  $\beta_{Cl}$  parameter was found to be 0.2 for the three-body decay channel which clearly differs from the value of 0.8 for the radical mechanism. Therefore, it was speculated that the two- and three-body decay channels occur on different upper states with the same A'' symmetry in agreement with the observations by Baum et al.<sup>10</sup> at 193 nm.

The present work extends the work of Roth et al.<sup>6,13</sup> to improve the knowledge on the photodissociation dynamics of SOCl<sub>2</sub> at 235 nm as we are now able to directly observe the full 3D product translational energy distribution and the dependence of the anisotropy parameter  $\beta$  on the fragment velocity which is of great importance in order to understand the dynamics. As a consequence mainly two overlapping decay mechanism were determined. One is a two-body decay releasing Cl and Cl\* in equal proportions with a  $\beta$  para-

meter of 0.76 together with internally cold  $\text{SOCl}$  partner fragments via an  $A''$  excited potential energy state (PES). On another PES, presumably of  $A'$  symmetry, two Cl atoms and one SO molecule are released in a three-body decay and in a two-body decay one Cl atom together with an internally excited  $\text{SOCl}^*$  radical is produced.

## 5.2 Experiment

A more detailed description of the experimental set-up and the novel position-sensitive detector (PSD) has been published elsewhere.<sup>1,4</sup> Briefly, it consists of a combination of a home-built single-field time-of-flight (TOF) mass-spectrometer and a position-sensitive detector.<sup>15-17</sup> The spectrometer was evacuated to a base pressure of about  $10^{-8}$  mbar by a turbo molecular pump system. Thionyl chloride was constantly cooled to  $-20^\circ\text{C}$  (gas pressure:  $\sim 15$  mbar at  $-20^\circ\text{C}$ ) to prepare a mixture of 0.5 %  $\text{SOCl}_2$  in helium. The mixture was fed into the spectrometer via a continuous supersonic beam. With a nozzle diameter of  $20\ \mu\text{m}$  and a stagnation pressure of ca. 3 bar typical working pressures were in the order of  $10^{-7}$  mbar. Under these conditions the beam is characterized by a rotational temperature of 8 K, determined by a rotationally resolved calibration spectrum of the NO ( $A^2\Sigma^+ \leftarrow X^2\Pi$ ) transition.<sup>1,18</sup>

Simultaneous dissociation and state-selective detection of chlorine atoms were performed using one dye laser pumped by a Nd:YAG laser (Coherent, Infinity 40-100). The dye laser (Lamba Physik, Scanmate) was operated with Coumarin 47 at a repetition rate of 100 Hz, its light was frequency doubled by a BBO crystal and focussed by a 20 cm lens in order to decrease the reaction volume to  $5 \cdot 10^{-4}\ \text{mm}^3$ . The energy of the frequency-doubled light was kept low ( $< 1\ \mu\text{J}$ ) to obtain approximately one fragment event per ten laser pulses to avoid kinetic energy transfer to the fragments due to space charge effects and saturation of the dissociation step. The laser beam, the molecular beam, and the detector axes were mutually orthogonal in the interaction region. Ultimate care was taken to overlap the light and the molecular beam which was checked frequently by monitoring of NO via (1+1) REMPI at 226 nm and optimizing the signal intensity.<sup>18</sup> The polarization of the laser was changed by a half wave plate in order to investigate the spatial fragment distribution. Typically the acceleration voltage was 800 V in the acceleration tube of the TOF spectrometer corresponding to an acceleration field of 16 kV/m.

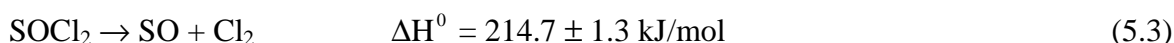
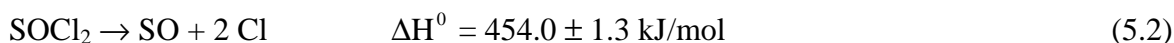
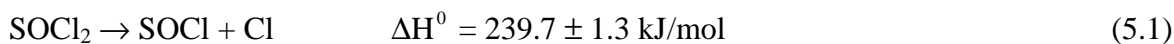
The  $^2P_J$  state of the chlorine atom is split by  $882\text{ cm}^{-1}$  due to spin orbit-coupling into  $\text{Cl}(^2P_{3/2})$  and  $\text{Cl}^*(^2P_{1/2})$ . Both states were detected by a (2+1) REMPI process. The ground state was probed via the ( $^2D_{3/2} \leftarrow ^2P_{3/2}$ ) transition at  $235.336\text{ nm}$ , the excited state by the ( $^2P_{1/2} \leftarrow ^2P_{1/2}$ ) transition at  $235.205\text{ nm}$ . Typically the dye laser was scanned over a range of  $\pm 0.003\text{ nm}$  around the Cl atom transition accounting for the Doppler broadening. Signals were processed by the electronic set-up, digitized by time-to-digital converters (TDCs), accumulated over  $2 \cdot 10^5$  laser shots, and saved on-line by a personal computer. The analyzing procedure is described in detail elsewhere.<sup>4</sup>

The PSD includes a delay-line anode (DLA) introduced into the spectrometer chamber right behind the double stage multi-channel plates (MCPs). The PSD allows us to monitor all three components of the momentum vector from the measured position of the particle on the detector and its arrival time. Therefore, a full 3D velocity distribution is observed and the complete information about the kinetic energy distribution and the velocity dependent  $\beta$  parameter is obtained.

## 5.3 Results and Discussion

### 5.3.1 Decay Channels

The one-photon dissociation of thionyl chloride can in principle proceed along one or several of the pathways (5.1-5.3). For a dissociation wavelength of  $235\text{ nm}$  the following reaction enthalpies are obtained for the spin-orbit states with the lowest energy:



The dissociation enthalpies were calculated from the standard enthalpies of formation ( $\Delta_f H^0$ )<sup>19</sup> of the molecules and radicals involved in the process and taken from ref. 7. The errors were calculated accordingly to the given errors of the individual standard enthalpies. The enthalpies were calculated for the spin-orbit ground state Cl. The  $\Delta H^0$  required for

formation of one or two Cl\* atoms is higher than the values given by 10.6 and 21.2 kJ/mol, respectively.

The molecular channel cannot be observed directly in our experiments. Whether it exists or not can only be decided by monitoring the energetics of the SO molecule or by direct observation of the molecular chlorine fragment as nascent particle. As the molecular channel was already well studied<sup>10,13</sup> and found to be of minor importance, we will not discuss the SO molecule in the present work.

### 5.3.2 Spin-Orbit Branching Ratio

The spin-orbit branching ratio was obtained by scanning the laser over the two resonance transitions of Cl and Cl\*. The measurements were repeated at different laser light intensities. Integrating the area under the Doppler profiles results in a signal ratio  $S(\text{Cl}^*)/S(\text{Cl})$  of  $0.5 \pm 0.04$ . Taking the ratio of transition probabilities  $B$  of  $1.06^{20}$  into account we determined a Cl\* yield  $\phi(\text{Cl}^*) = 0.35 \pm 0.03$  where  $\phi$  is defined as the ratio of the number of excited state atoms  $P(\text{Cl}^*)$  to the total number of chlorine atoms:  $\phi(\text{Cl}^*) = P(\text{Cl}^*)/[P(\text{Cl})+P(\text{Cl}^*)]$ . This value is in perfect agreement with both branching ratios given by Roth et al.<sup>6,13</sup> ( $\phi(\text{Cl}^*) = 0.35 \pm 0.05$ ) and Kawasaki et al.<sup>12</sup> ( $\phi(\text{Cl}^*) = 0.37$ ). In the latter case the published value was readjusted due to the most recently observed transition probabilities for the Cl spin-orbit states.<sup>20</sup> Although the value of 0.35 coincides with the value of a statistical distribution (0.33), it does not mean that the decay proceeds statistically. On the contrary, the value of 0.35 is obtained only from averaging over several highly non-statistical decay channels. This fact illustrates the necessity to monitor the decay dynamics in the greatest detail possible.

### 5.3.3 Speed Dependence of the Spatial Fragment Distribution

Previously, experiments were mainly performed under conditions where the speed distribution could only be determined in one dimension and there was no possibility to directly measure the speed dependence of the anisotropy parameter  $\beta$ . As we are able to observe the three-dimensional (3D) momentum vector of a single reaction product we turned our attention to the observation of the speed dependence of the  $\beta$  parameter. In Fig. 5.2 the speed distributions and the speed dependent  $\beta$  parameters for Cl and Cl\* are presented. This 1D presentation is obtained by integration of the 3D data. Although both distributions are bimodal, a remarkably different behavior of the two spin-orbit components with respect to their kinetic energy acquisition in the photodissociation is obvious. The distribution of the ground state Cl is of double peak shape, with the peaks at 900 and 2500 m/s separated by a minimum at 1800 m/s. The first peak at 900 m/s is more intense than the second at 2500 m/s by a factor of 1.2. In the case of excited state Cl\* the distribution is singly peaked at 2500 m/s, accompanied by a tail only in the low speed region around 1200 m/s. The small shoulders above 3500 m/s belong to a small contribution of  $^{37}\text{Cl}$ . These observed distributions are in brilliant agreement with the results obtained by Roth et al.<sup>6,13</sup> via 1D REMPI-TOF measurements and by Kawasaki et al.<sup>12</sup> via ion imaging.

Noteworthy is the speed dependence of the  $\beta$  parameter. In the case of ground state Cl the  $\beta$  parameter belonging to particles with low speed is only slightly positive which means that the slow ground state Cl fragments are almost isotropically distributed whereas in the region of high speed the  $\beta$  parameter increases to  $0.85 \pm 0.1$ . It is important to note that the strong  $\beta$  parameter increase is shifted from the observed speed distribution minimum at 1800 m/s and the energetic limit for the three-body decay at 1500 m/s by 300 m/s and 600 m/s, respectively, towards the higher recoil speeds. In the case of excited state Cl\* the anisotropy behavior is very similar to the ground state Cl anisotropy. At 2100 m/s the value of the  $\beta$  parameter increases rapidly to a value of  $0.68 \pm 0.1$ . Analogously to ground state Cl the increase of the  $\beta$  parameter is shifted with respect to the increase in intensity and the energetic limit for the three-body decay.

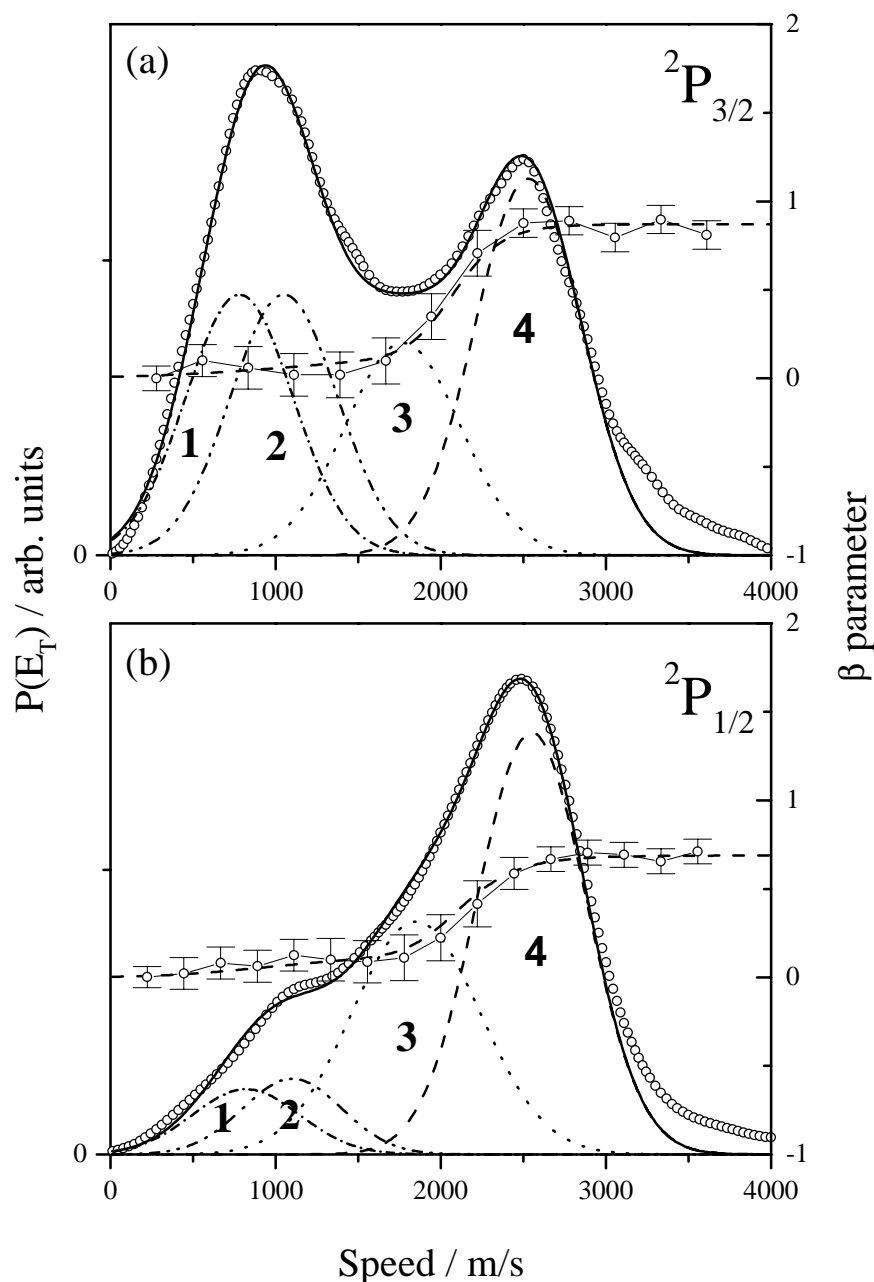


**Figure 5.2:** Speed distribution for (a) ground state  $\text{Cl}(^2P_{3/2})$  and (b) excited state  $\text{Cl}^*(^2P_{1/2})$  atoms produced in the photodissociation of  $\text{SOCl}_2$  at 235 nm. The dependence of the  $\beta$  parameter on the Cl fragment kinetic energy (right scale) is shown by curves with error bars.

For both Cl and  $\text{Cl}^*$  the speed distribution is bimodal divided in a region of high speed with a strong positive  $\beta$  parameter and a low speed region with a slightly positive  $\beta$  parameter. In order to elucidate the different decay mechanism, four Gaussian are fitted to the bimodal distribution, since the three-body decay can not account for the region with the slightly positive

$\beta$  parameter up to 1800 m/s solely, as its energetic limit is at 1500 m/s. Thus, the slow speed region is divided into three parts accounting for a sequential three-body decay [1(dash dotted line) and 2(dash dot dotted line)] and a two-body decay [3(dotted line)] releasing intermediate fast Cl and highly excited SOCl\*. The fourth Gaussian describes fast chlorine fragments [4(dashed line)] produced together with internally cold SOCl radicals in a two-body decay characterized by a  $\beta$  parameter of 0.85 and 0.68 for Cl and Cl\*, respectively.

Taking the bimodal structure of the speed distribution and the  $\beta$  parameter speed dependence into account, at least two competing decay mechanisms of the parent molecule are postulated. Fast Cl and Cl\* with a non-vanishing  $\beta$  parameter are released in a two-body decay, whereas slow, predominantly ground state Cl atoms with an almost isotropic distribution are released via a three-body decay. Since the three-body decay can not account for the intermediate fast Cl atoms above 1500 m/s with a  $\beta$  parameter of 0.1, this speed region must be further subdivided.

First, as the simpler case, the two-body decay shall be discussed. According to the observed  $\beta$  parameter increase at about 2000 m/s, one Gaussian is fitted to the high speed region accounting for the two-body decay generating Cl and Cl\* with high kinetic energy and a  $\beta$  value of 0.85 and 0.68, respectively. The mean centers of the Gaussians are at 2540 m/s with a mean widths of 655 m/s. The probability that Cl or Cl\* will be released is  $\phi(\text{Cl}^*) = 0.4$ .

The observed values of 0.68 and 0.85 are close to the theoretical limit of 0.7 for the  $\beta$  parameter for an instantaneous decay from the ground state geometry with a Cl-S-Cl bond angle of 97°, as shown in Fig. 5.3. Hence the symmetry of the excited surface is of A" symmetry and the transition dipole moment  $\mu$  is oriented parallel to the line connecting the two Cl atoms (perpendicular to the plane of symmetry).

The measured  $\beta$  value above the theoretical limit may hint at an excited surface with an increased Cl-S-Cl bond angle. Under molecular beam conditions, a  $\beta$  value close to the limiting value is evidence of a fast bond cleavage within less than 200 fs where a Cl or Cl\* atom with high kinetic energy is released. The upper limit of the dissociation time is calculated from Wilson.<sup>21</sup>

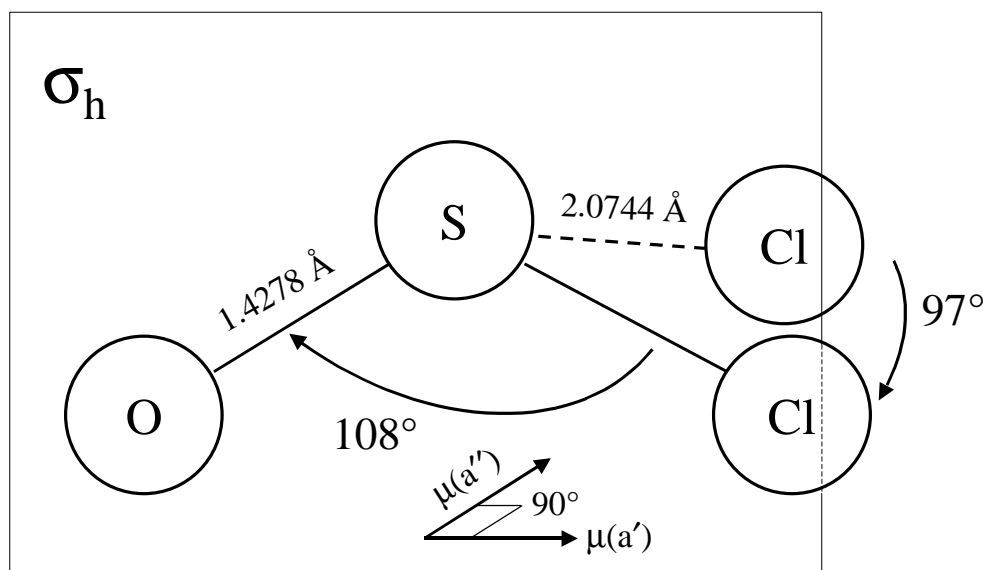


**Figure 5.3:** Geometry of SOCl<sub>2</sub> molecule, both transition dipole moments  $\mu$  ( $a'$ ) in the plane of the symmetry and  $\mu$  ( $a''$ ) perpendicular to the plane of symmetry are presented.

The electronic configuration of the SOCl<sub>2</sub> molecule confirms the assumption of an excited electronic state of A'' symmetry. The sulfur atom in the molecule is sp<sup>3</sup> hybridized. Two of these hybrid orbitals are singly occupied and build a  $\sigma_{\text{S-Cl}}$ -bonding with the singly occupied p-orbitals of the chlorine atoms. One of the residual doubly occupied hybrid orbitals is oriented on top of the S-atom so that it describes a tetrahedron together with the SO- and SCl-bondings. In case of the  $\pi_{\text{S-O}}$ -bonding one electron of the last hybrid orbital is excited to a d-orbital and then combined with a p-orbital of the O-atom, while the electron remaining in the hybrid orbital generates the  $\sigma_{\text{S-O}}$ -bonding with the second p-orbital of the oxygen atom. Neglecting the inner-shell electrons of the atoms and assuming the  $\pi_{\text{S-O}}$ -bonding lying in the symmetry plane  $\sigma_{\text{h}}$  the electronic configuration of the molecule is described by

$$\dots \underbrace{(7a'')^2(11a')^2(12a')^2(13a')^2}_{\text{bondings}} \underbrace{(8a'')^2(14a')^2(15a')^2}_{n_{\text{O}}, n_{\text{Cl}}(3s)} \underbrace{(9a'')^2(16a')^2(17a')^2}_{n_{\text{Cl}}(3p)} \underbrace{(10a'')^2(11a'')^2(18a')^2}_{n_{\text{S}}}.$$

The non-bonding outer-shell orbitals of the atoms are labelled with *n*. In parentheses the symmetry of the orbitals in respect to C<sub>s</sub> symmetry group is added. Orbitals with the same symmetry are serially numbered. Although the assignment to the atoms is arbitrary and not connected with their energetic order it is clear that the highest occupied molecular orbital (HOMO) is the non-bonding n<sub>s</sub>(a')-orbital. The lowest unoccupied molecular orbital (LUMO) is the anti-bonding π\*<sub>SO</sub>(a')-orbital.<sup>8</sup> The lowest electronic transition π\*<sub>SO</sub>(a') ← n<sub>s</sub>(a') leads to an excited state of A' symmetry as observed in the photodissociation at 248 nm. At 235 nm the transition σ\*<sub>SO</sub>(a'') ← n<sub>s</sub>(a') is predominant leading to an excited state of A'' symmetry, the contribution of different transitions from the n<sub>Cl</sub> orbitals increase with increasing photolysis energy resulting in additional states of both A' and A'' symmetry.

Generally, the low speed region may be divided into two parts by simple energetic considerations. Due to the dissociation energy, Cl atoms which are released via a three-body decay cannot receive speeds above 1500 m/s. Thus, atoms faster than 1500 m/s are released in a second two-body decay mechanism together with an internally excited SOCl\*. This channel is characterized by a slightly positive β parameter of 0.1. This observations are in agreement with a highly excited SOCl\* at 9000 cm<sup>-1</sup> examined by Baum et al.,<sup>10</sup> although Baum et al. did not observe a different anisotropy for the two different two-body decays. This is probably due to the low influence of the second two-body decay at 248 nm. According to the observed β parameter of 0.1, it is most likely that the intermediate fast Cl are released via an excited state of A' symmetry. The theoretical limit of the β parameter for an instantaneous decay on an excited surface of A' symmetry is 0.3 and the transition dipole momentum μ is lying in the plane of symmetry, as shown in Fig. 5.3. Thus, one Gaussian is fitted to the intermediate speed range accounting for the second two-body decay. The Gaussians for Cl and Cl\* are almost identical and a mean value of 1810 m/s for the center at a mean widths of 640 m/s is obtained.

Hence, two different two-body decay mechanisms are determined releasing firstly fast Cl plus internally cold SOCl (curve 4 in Fig. 5.2) and generating secondly Cl in conjunction with an internally excited SOCl\* (curve 3 in Fig. 5.2). The ratio between the two different two-body mechanism is about 1.5:1 for the first (curve 4) and the second (curve 3), respectively. The ratio is identical for both Cl and Cl\*.

In the case of the three-body decay different observations were previously made. At 193 nm Baum et al.<sup>10</sup> postulated an asynchronous concerted decay with a positive  $\beta$  parameter of 0.43 which is in good agreement with their observed  $\beta$  parameter of 0.4 for the two-body decay. Kawasaki et al.<sup>12</sup> observed at 235 nm an isotropic distribution (i.e.  $\beta \approx 0$ ) of slow Cl and Cl\* atoms. Roth et al.<sup>6,13</sup> observed an averaged  $\beta$  parameter of 0.2 at 235 nm and postulated a sequential decay, where the first Cl is released with a positive  $\beta_{\text{Cl}}$  and the second one is isotropically distributed as the  $\beta_{\text{SO}}$  was found to be zero. Therefore, the observable  $\beta_{\text{Cl}}$  parameter is an average between the positive  $\beta$  value of the first step and the isotropic distribution of the second step. A different behavior at 193 nm and 235 nm may be explained by the additional available energy which can reduce the decay time and may change the mechanism from sequential to asynchronous concerted.

In the three-body range, a single Gaussian fit could not describe the speed distribution with its speed dependent  $\beta$  parameter satisfactorily. Thus, two Gaussians were fitted to the experimental data supported by the sequential decay postulated by Roth et al. The mean centers of the Gaussians are at 800 m/s and 1075 m/s with mean widths of 625 m/s and 650 m/s for slow and intermediate slow chlorine atoms, respectively. Since the two Gaussians almost overlap it is suggested that the decay mechanism is at the border between a sequential decay and an asynchron-concerted one. In the three-body region the probability that Cl\* will be released is rather small:  $\phi(\text{Cl}^*) = 0.23$ . The observed  $\beta$  parameter is about 0.1 for the Cl being generated in the first step and close to zero for the Cl released in the second step. Detailed data describing the kinetics are given in Table 5.1.

The observed identical values for the  $\beta$  parameters for the slow two-body decay fragments (curve 3 in Fig. 5.2) and the fast three-body decay fragments (curve 2 in Fig. 5.2) suggest that these fragments are generated on the same upper potential energy surface of A' symmetry. Baum et al. assigned the surface to be of A'' symmetry on which the three-body decay occurs at 193 nm due to the observed  $\beta$  parameter of 0.4.<sup>10</sup> The different observations are probably due to the different photolysis energies since many states may be accessed below 200 nm.

**Table 5.1:** Characteristic data describing the speed distribution, the  $\beta$  parameter of the Cl and Cl\* fragments, and the kinetic energy release in the photodissociation of SOCl<sub>2</sub>. The kinetic energy release is obtained for the two- (2BD) and three-body decay (3BD) separately. The analysis consists of four Gaussians assuming two different kinds of 2BDs and a sequential 3BD.

Fragment	Type	Decay channel		$E_{av}$ (kJ/mol)	$\langle E_T \rangle$ (kJ/mol)	$\langle E_T \rangle / E_{av}$
Cl	2BD		SOCl <sub>2</sub> → SOCl + Cl	269	112	0.42 ± 0.03
	2BD		SOCl <sub>2</sub> → SOCl* + Cl		55	0.20 ± 0.03
	3BD	(a)	SOCl <sub>2</sub> → SOCl + Cl	54	15	0.28 ± 0.03
		(b)	SOCl → SO + Cl			
Cl*	2BD		SOCl <sub>2</sub> → SOCl + Cl*	258	114	0.44 ± 0.03
	2BD		SOCl <sub>2</sub> → SOCl* + Cl*		60	0.23 ± 0.03
	3BD	(a)	SOCl <sub>2</sub> → SOCl + Cl*	43	16	0.37 ± 0.03
		(b)	SOCl → SO + Cl*			

Fragment	Type	Percentage (%)	$\beta$ Parameter	Analysis	
				Peak (m/s)	FWHM (m/s)
Cl	2BD	28.3	0.85 ± 0.08	2530	650
	2BD	17.2	0.10 ± 0.13	1770	700
	3BD	19.5	0.10 ± 0.12 0.00 ± 0.07	1050 780	650 650
Cl*	2BD	19.2	0.68 ± 0.07	2550	660
	2BD	12.6	0.10 ± 0.13	1850	680
	3BD	3.2	0.10 ± 0.12 0.00 ± 0.06	1100 820	650 600

Hence, a more refined picture of the decay dynamics is obtained. Instead of associating the three-body decay channel and the two-body decay channel with different excited states, we conclude that an A' state predominantly produces three fragments via reaction (5.2) and

two fragments via reaction (5.1) where the  $\text{SOCl}$  fragments are highly internally excited. The latter fragments are likely to carry predominantly vibrational and rotational energy and can be associated with those fragments previously suggested to be produced in a hitherto unobserved electronically excited state.<sup>10</sup> Fast  $\text{Cl}$  fragments in both spin-orbit states are generated on an excited state of  $A''$  symmetry via a fast and direct dissociation. Both  $A''$  and  $A'$  surfaces can be associated with the promotion of a non-bonding electron at the sulfur and the chlorine atoms, respectively, to the anti-bonding  $\sigma^*_{\text{SCl}}$  molecular orbital.<sup>6,8</sup> Thus, the dissociation is expected to be fast on both surfaces. For the molecular channel (5.3) previous experiments suggested the dissociation to proceed via an  $A'$  surface which is to be associated with the promotion of a non-bonding electron at the sulfur atom into the  $\pi^*_{\text{SO}}$  molecular orbital.<sup>6,8</sup>

## 5.4 Conclusions

The photodissociation of  $\text{SOCl}_2$  at 235 nm was studied by a novel REMPI-TOF 3D imaging technique. Both ground and excited chlorine are produced with a total yield of  $\phi(\text{Cl}^*) = 0.35$ . The dissociation is highly spin selective with spin-orbit state specific bimodal kinetic energy distributions. The speed dependence of the anisotropy parameter  $\beta$  was observed for the first time in detail and yields new insight into the complex fragmentation behavior of  $\text{SOCl}_2$ . A sudden change of the  $\beta$  parameter value from 0.15 to 0.76 at intermediate kinetic energy for both ground and excited state  $\text{Cl}$  and  $\text{Cl}^*$  fragments is evidence of mainly two overlapping decay mechanisms. The first (low  $\beta$  value) manifests itself both as a three-body decay producing two chlorine atoms and one  $\text{SO}$  molecule and as two-body decay generating a  $\text{Cl}$  atom in conjunction with an internally excited  $\text{SOCl}^*$  radical via an excited potential energy surface of  $A'$  symmetry. The second ( $\beta = 0.76$ ) is a two-body decay releasing fast  $\text{Cl}$  and  $\text{Cl}^*$  atoms in equal proportions together with internally cold  $\text{SOCl}$  partner fragments via an  $A''$  excited potential energy surface.

## 5.5 Acknowledgement

The authors are grateful to Dr. M. Roth for numerous stimulating discussions. These studies were supported by the Fonds der Chemischen Industrie, the Alexander von

---

Humboldt Stiftung, and the German-Israeli Foundation (GIF). Financial support by the Deutsche Forschungsgemeinschaft is gratefully acknowledged.

---

- <sup>1</sup> A. Chichinin, T. Einfeld, C. Maul, and K.-H. Gericke, *Rev. Sci. Instr.* **73**, N4, xxx (2002).
- <sup>2</sup> T. Einfeld, A. Chichinin, C. Maul, and K.-H. Gericke, *J. Chem. Phys.* (in press).
- <sup>3</sup> C. Maul, T. Haas, K.-H. Gericke, *J. Chem. Phys.* **102**, 3238 (1995); C. Maul, T. Haas, K.-H. Gericke, *J. Phys. Chem. A* **101**, 6619 (1997).
- <sup>4</sup> T. Einfeld, A. Chichinin, C. Maul, and K.-H. Gericke, *J. Chem. Phys.* **116**, 2803 (2002).
- <sup>5</sup> A. P. Uthmann, P. J. Demlein, T. D. Aliston, M. C. Withiam, M. J. McClements, and G. A. Takacs, *J. Phys. Chem.* **82**, 2252 (1978).
- <sup>6</sup> M. Roth, C. Maul, and K.-H. Gricke, submitted to *Phys. Chem. Chem. Phys.*
- <sup>7</sup> R. J. Donovan, D. Husain and P. T. Jackson, *Trans. Faraday Soc.* **65**, 2930 (1969).
- <sup>8</sup> M. Kawasaki, K. Kasatani, H. Sato, H. Shinohara, N. Nishi, H. Ohtoshi and I. Tanaka, *Chem. Phys* **91**, 285 (1984).
- <sup>9</sup> C. Maul and K.-H. Gericke, *Int. Rev. Phys. Chem.* **16**, 1 (1997).
- <sup>10</sup> G. Baum, C. S. Effenhauser, P. Felder, and J. R. Huber, *J. Phys. Chem.* **96**, 756, 1992.
- <sup>11</sup> M. Bogey, S. Civis, B. Delcroix, C. Demuyneck, A. F. Krupnov, J. Quiguer, M. Yu. Tretyakov, and A. Walters, *J. Mol. Spectrosc.* **182**, 85 (1997).
- <sup>12</sup> M. Kawasaki, K. Suto, Y. Matsumi, and R. Bersohn, *J. Phys. Chem.* **100**, 19853 (1996).
- <sup>13</sup> M. Roth, *Untersuchung photoindizierter Dreikörperzerfälle am Beispiel von  $\text{Cl}_2\text{O}$  und  $\text{SOCl}_2$* , PhD thesis, Univ. Braunschweig (2000).
- <sup>14</sup> Z. Li, *J. Phys. Chem. A* **101**, 9545 (1997).
- <sup>15</sup> S. E. Sobottka and M. B. Williams, *IEEE Trans. Nucl. Science* **35**, 348 (1988).
- <sup>16</sup> O. Jagutzki, V. Mergel, K. Ullmann-Pfleger, L. Spielberger, U. Meyer, R. Dörner, and H. Schmidt-Böcking, *Fast position and time-resolved read-out of micro-channel plates with the delay-line technique for single particle and photon detection*, Imaging spectroscopy IV, 322, San Diego, California (1998).
- <sup>17</sup> M. Lampton, O. Siegmund, and R. Raffanti, *Rev. Sci. Instr.* **58**, 2298 (1987).
- <sup>18</sup> J. Danielak, U. Domin, R. Kepa, M. Rytel, and M. Zachwieja, *J. Mol. Spectrosc.* **181**, 394 (1997).
- <sup>19</sup> M. W. Chase, NIST-JANAF, Thermochemical Tables, Fourth Edition, *J. Phys. and Chem. Reference Data*, Monograph 9, Part I + II (1998).
- <sup>20</sup> P. M. Regan, S. R. Langfold, D. Ascenzi, P. A. Cook, A. J. Orr-Ewing, M. N. R. Ashfold, *Phys. Chem. Chem. Phys.* **1**, 3247 (1999).
- <sup>21</sup> G. E. Busch and K. R. Wilson, *J. Chem. Phys.* **56**, 3638 (1972).